Water Research X 27 (2025) 100306

Contents lists available at ScienceDirect

Water Research X

journal homepage: www.sciencedirect.com/journal/water-research-x

Evaluation of nitrous oxide reduction in solid carbon source-driven counter-diffusional biofilm denitrification system

Yingrui Liu [a,1], Feng Chen [a,1], Yanying He [a], Yufen Wang [a], Tingting Zhu [a,*], Yindong Tong [a], Yingxin Zhao [a], Bing-Jie Ni [b], Yiwen Liu [a,*]

[a] School of Environmental Science and Engineering, Tianjin University, Tianjin 300072, PR China
[b] School of Civil and Environmental Engineering, University of New South Wales, Sydney, New South Wales, 2052, Australia

ARTICLE INFO

Keywords:
Nitrous oxide (N2O)
Polycaprolactone (PCL)
Counter-diffusional biofilm
Solid carbon source
Solid-phase denitrification (SPD)

ABSTRACT

Solid carbon-driven biofilm system can provide sufficient carbon source for denitrification, while its counter-diffusional structure could inevitably induce the delayed carbon-nitrogen contact and electron transport, further affecting carbon footprints mainly contributed by nitrous oxide (N_2O) at wastewater treatment plants (WWTPs). However, the detailed understanding of N_2O dynamics during solid-phase denitrification (SPD) has not been disclosed. In this work, a fixed bed bioreactor driven by polycaprolactone (PCL) was constructed and operated over 180 days, achieving 97 %-99 % of total nitrogen (TN) removal efficiency. Biochemical results indicated that under the condition that each nitrogen oxide (NO_x) concentration was maintained at 30 mg-N/L, the electron competition between upstream and downstream electron pools was still observed during PCL-driven denitrification even providing sufficient carbon source. For example, under the coexistent nitrate (NO_3^-)+ nitrite (NO_2^-)+N_2O condition, few electrons (i.e., 12.6 %) distributed to N_2O reductase (*Nos*), significantly decreasing the N_2O reduction rate (i.e., 1.42 mg/g VSS/h). Under the condition that TN concentration was maintained at 30 mg-N/L, the TN removal rate in the scheme containing NO_3^-+NO_2^-+N_2O was observed to be 1.75–2.3 times higher than that of the scheme with sole NO_x of 30 mg-N/L. This suggested that when treating wastewater containing multiple NO_x, the PCL-driven biofilm denitrification system can not only relatively improve the total nitrogen removal efficiency, but also relatively alleviate N_2O emissions. The higher abundance of *Bacteroidota* and *Comamonadaceae* ensured the stable carbon source release and nitrogen conversion states.

1. Introduction

Wastewater treatment plants (WWTPs) typically remove nitrate or nitrite through denitrification processes to avoid the negative effects of excess nitrogen on aquatic ecosystems (Duan et al., 2021; Hatzikioseyian et al., 2023). Among physical, chemical, and biological methods, the biological approach is deemed the most effective and promising (Zhang et al., 2025). Biological denitrification can be categorized as two metabolic pathways, namely heterotrophic and autotrophic processes, with the former being the more common and practical pathway, offering the advantages of high efficiency and low treatment cost (Fu et al., 2022; Hu et al., 2023). In general, heterotrophic denitrification occurs under anaerobic or anoxic conditions through biological heterotrophic reduction, during which denitrifying bacteria complete the denitrification process by consuming organic substrates to obtain sufficient electrons (Fang et al., 2020). Complete heterotrophic denitrification is the successive reduction of nitrate (NO_3^-)→nitrite (NO_2^-)→nitric oxide (NO)→nitrous oxide (N_2O)→nitrogen gas (N_2) with the participation of various reductases (Zheng et al., 2024). Imbalances in the reduction rates of adjacent denitrification steps, i.e., changes in external factors such as the limited available carbon sources, would result in the accumulation of specific nitrogen oxide intermediates.

Liquid carbon sources such as sodium acetate, glucose, and methanol mainly collected through sludge treatment are the most commonly used electron donors for heterotrophic denitrification (Liu et al., 2022; Wang et al., 2024a; Wang et al., 2022b). However, water-soluble organic matter could carry the risk of insufficient or excessive dosage in operation and toxicity or flammability during storage and transportation, as well as require complex monitoring and control process. In contrast to conventional liquid carbon sources, solid carbon sources exhibit the

* Corresponding authors.
E-mail addresses: ttzhu@tju.edu.cn (T. Zhu), yiwen.liu@tju.edu.cn (Y. Liu).
[1] Yingrui Liu and Feng Chen contributed equally to the work.

https://doi.org/10.1016/j.wroa.2025.100306
Received 30 November 2024; Received in revised form 16 January 2025; Accepted 22 January 2025
Available online 22 January 2025

advantages of easy management, infrequent addition, low sludge yield, controllable carbon release, and appreciable denitrification rate (Zhang et al., 2022a). In this regard, solid-phase denitrification (SPD) has been considered as a promising alternative technology. Solid carbon sources comprise synthetic biodegradable polymers and natural materials, with the former allowing for higher denitrification efficiency and more stable effluent quality (Chu and Wang, 2013). Solid carbon sources can serve as both the electron donor and biofilm carrier, thus leading to the unique counter-diffusional mass transfer behavior. The dense biofilm that grows and attaches to the polymer surface provides a protective zone for the internal denitrifiers, thereby enhancing the resilience of functional bacteria to shock loadings (Fu et al., 2022). Among the various biodegradable polymers, polycaprolactone (PCL) is the most widely studied and applied with respect to better bioavailability and more attractive economics (Zhang et al., 2022a).

During biological nitrogen removal in wastewater treatment, N_2O, the intermediate product of denitrification with global warming potential of approximately 300 times greater than that of carbon dioxide (CO_2), is inevitably produced (Liu et al., 2025). N_2O has caused profound negative impacts on the ozone layer for its high global warming potential and long lifetime (Dai et al., 2021). It has been indicated that in recent decades, atmospheric N_2O concentration has increased at an average rate of 0.26 % per year (Huang et al., 2023). Reportedly, N_2O accounted for ca. 23 % of the direct emissions from total wastewater treatment plants worldwide (He et al., 2023a). Denitrification could act as both a source and sink of N_2O (Tong et al., 2024). Therefore, understanding the pathway of N_2O production and controlling the denitrification process as an effective N_2O sink rather than a net source is considered crucial opportunities to reduce the greenhouse effect and carbon footprint (He et al., 2023b; He et al., 2024b). Regarding N_2O production during the SPD process, Liu et al. (2019) observed N_2O accumulation in an aerobic granular sludge (AGS) pre-reactor and a poly (butylene succinate)-supported SPD post-reactor. However, little is known about the dynamics of N_2O production during SPD.

The aim of this study was to investigate the N_2O turnovers (i.e., production and consumption) under different combinations of electron acceptors and different nitrogen loading conditions in a counter-diffusion biofilm system represented by PCL. An upflow fixed-bed reactor was constructed and operated for >180 days to form a stable biofilm on the surface of the solid carbon source, followed by multiple sets of batch experiments and microbial characterization. In addition, this study provided an inner-cycle mode method that can be used to determine the cyclic variation of N_2O in granular counter-diffusion biofilms.

2. Results and discussion

2.1. SPD reactor performance

Since the amount of organic carbon released from solid carbon sources is regulated by bacteria that respond to bulk nitrate concentration, SPD systems can be considered as non-carbon-limiting conditions. An up-flow fixed bed reactor was operated for a period of 180 days. The denitrification performance of the reactor and the characteristic of the synthetic wastewater were presented in Fig. 1 and **Table S1**, respectively. Stable NO_3^- removal rates were obtained within the first 15 days, after which a long operation period was taken for biofilm formation, development, and stabilization on the PCL pellets surface. The total nitrogen removal efficiency was above 97 % at 154–180 days, indicating a higher denitrification performance.

2.2. Electron competition

Fig. 2**A-G** showed the variation of nitrogen oxide (NO_x) profiles, which was based on the data of the first 1 h in schemes A-G (Table 1). Schemes A-C represented the sole NO_3^-, NO_2^- and N_2O addition,

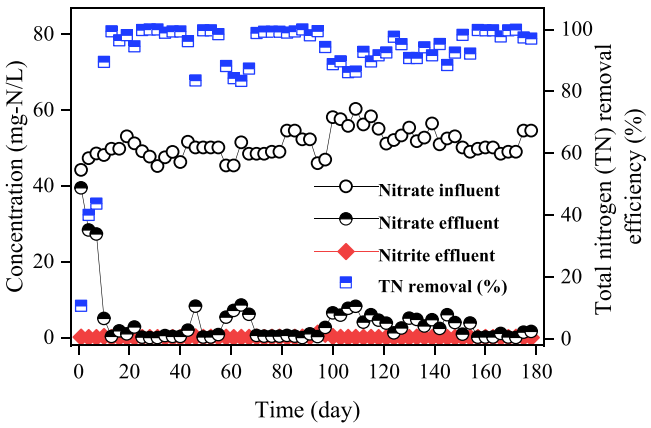

Fig. 1. The performance of the up-flow solid-phase denitrification reactor during 180 days of operation.

respectively. Schemes d-F represented NO_3^-+NO_2^-, NO_3^-+N_2O, NO_2^-+N_2O and NO_3^-+NO_2^-+N_2O, respectively. Each NO_x concentration in each scheme was 30 mg-N/L. The profiles of NO_3^-, NO_2^- and N_2O in schemes A-C and E were displayed a linearly downward trend, which was consistent with previous study (Liu et al., 2022). Notably, the rate of decreasing NO_3^- levels in schemes D and G (i.e., both NO_3^- and NO_2^- were present simultaneously) was higher than the rate observed in scheme A. Additionally, the NO_2^- level remained almost constant at ca. 25 mg-N/L, indicating that the reduction of NO_3^- to NO_2^- occurred at a rate approximately equal to the NO_2^- consumption rate. In scheme E (i.e., NO_3^-+ N_2O), NO_3^- and N_2O concentrations decreased by 8.5 and 3.5 mg-N/L, respectively. While, the N_2O level increased by ca. 2.8 mg-N/L in scheme F (i.e., NO_2^-+ N_2O).

In Fig. 3**A**, the net NO_3^-, NO_2^-, and N_2O reduction rates were 0.84, 2.25, and 1.66 mg N/g VSS/h, respectively. In schemes D and G (i.e., NO_3^- and NO_2^- simultaneously existed), the NO_3^- reduction rate was obviously the highest (i.e., 2.58 and 2.62 mg/g VSS/h, respectively). In schemes F and G (i.e., NO_2^- and N_2O simultaneously existed), the NO_2^- reduction rate (3.76 and 2.6 mg/g VSS/h, respectively) was apparently higher than the N_2O reduction rate (2.81 and 1.35 mg/g VSS/h, respectively).

In Fig. 3**B**, the electron consumption rates of each reductase corresponding to NO_x reduction rates were calculated (Pan et al., 2019). During scheme A, NO_2^-, NO, and N_2O were formed as denitrifying intermediates. The highest electron consumption rates were observed for *Nar* (0.11 mmol e/g VSS/h) in scheme A, *Nir* (0.16 mmol e/g VSS/h) in scheme B, and *Nos* (0.1 mmol e/g VSS/h) in scheme C. This result indicated that electron competition inevitably occurred in all tests when the potential electron consumption rate (PEC) exceeded the maximum electron supply rate (MES) according to previous study. The total electron consumption rate in the multiple NO_x schemes was significantly higher than that in the sole NO_x schemes. It was in agreement with the results observed in previous studies of both forward-diffusion and counter-diffusion biofilm systems (Pan et al., 2019; Roy et al., 2021), suggesting that the PCL-driven SPD system consistently and steadily provided sufficient carbon sources for NO_x reduction. However, the N_2O reduction rate and the electron consumption rate of *Nos* were consistently the lowest. This was likely due to electron competition between the upstream electron pool (i.e., the quinol pool, where electrons were directly utilized by *Nar*) and the downstream electron pools (i.e., periplasmic small c-type cytochromes, which accepted electrons from the quinol pool and then transfer them to *Nir* and *Nos* via the bc1 complex) (Liu et al., 2025), electrons diffusing from inner to outer layer allocated to *Nos* was the least.

Fig. 3**C** illustrated the electron distribution patterns among *Nar, Nir*, and *Nos* in schemes D, E, F and G in the PCL-driven SPD system. Obviously, electrons consistently tended to flow toward *Nar* (35.1–48.5 %),

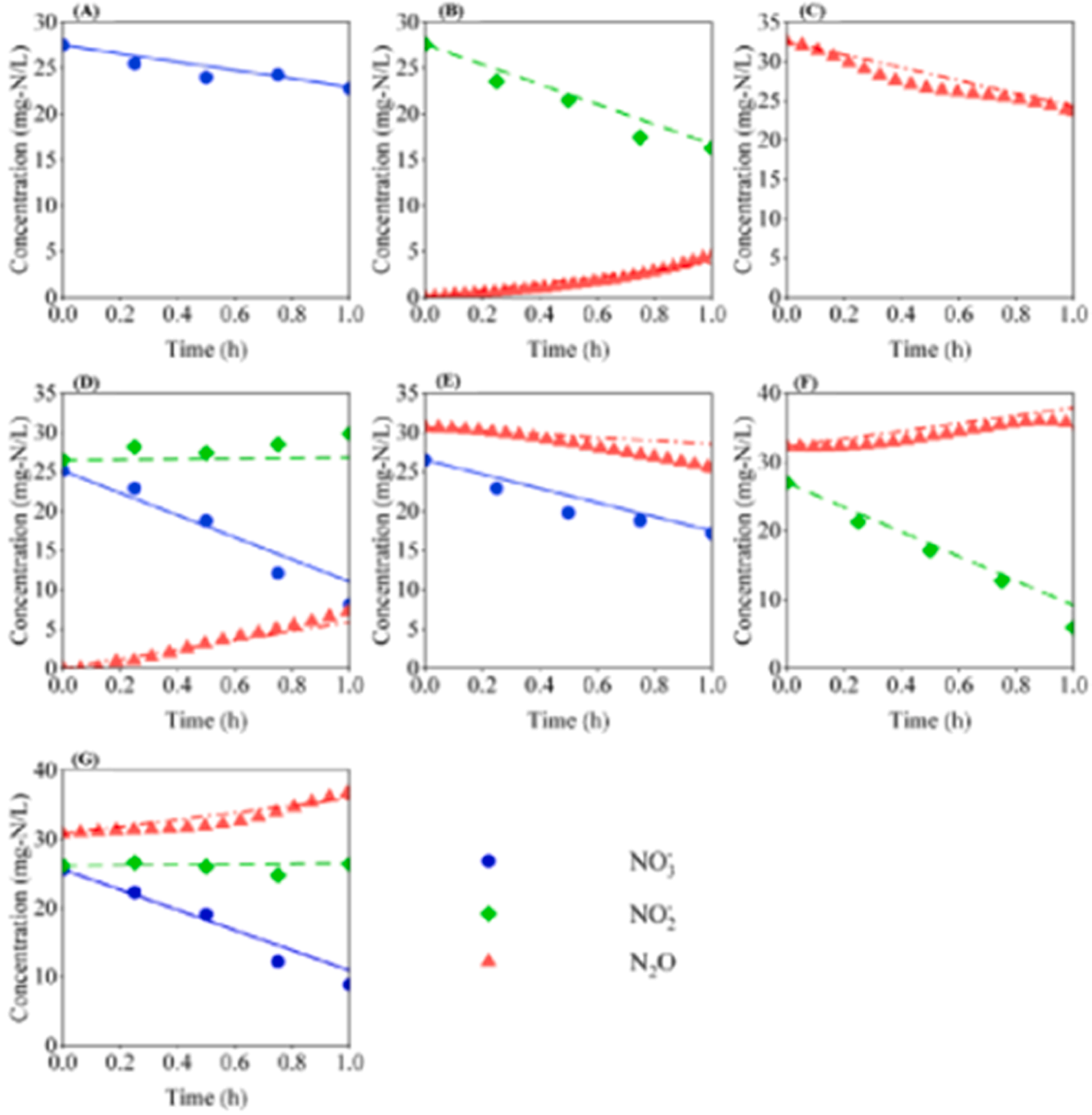

Fig. 2. NO_3^-, NO_2^- and N_2O profiles during electron competition experiment from the PCL-supported biofilm denitrification system.

confirming the above results (Fig. 3**A** and 3**B**) that electrons preferentially flowed toward the upstream electron pool. Compared to schemes E and F, more electrons flowed toward *Nar* in scheme G, indicating electron competition between the upstream and downstream electron pools. Overall, electron competition between the two electron pools was the primary reason for the lower N_2O reduction rate in the PCL-driven SPD system.

2.3. NO_x reduction and N_2O accumulation in the PCL-driven spd system

Figs. 4–6 demonstrated the variations of NO_x levels during the 2–4 h batch tests in 11 schemes, which contained sole and multiple NO_x addition schemes (i.e., A-G) with each NO_x concentration of 30 mg-N/L, and multiple NO_x addition schemes (i.e., H-K) with TN concentration of 30 mg-N/L (Table 1). In Fig. 4, the concentrations of NO_3^-, NO_2^-, or N_2O decreased by 21.2, 25.3 and 29.9 mg-N/L within 4.0 h, 2.75 h and 3.5 h, respectively. The reduction rates were consistent with the results from the first hour (Fig. 2 and 3**A**). In Fig. 4**B**, the N_2O concentration initially showed an increasing trend, followed by a decreasing trend at 2.75 h, and the maximum accumulation N_2O concentration exceeding 10 mg-N/L. This indicated that electrons were utilized by *Nos* for the N_2O reduction as NO_2^- was consumed, further highlighting the electron competition between downstream electron pools (Fig. 3**C**). Similar N_2O accumulation has been observed in a previous powdered degradable microplastic-activated sludge system (He et al., 2024a). The possible reason was that PCL may significantly reduce the relative abundance of

Table 1
Electron acceptors addition scheme.

Data set 1		A	B	C
Electron acceptor added		NO_3^-	NO_2^-	N_2O
Added concentration		30	30	30
Total NOx concentration		30	30	30
Data set 2	**D**	**E**	**F**	**G**
Electron acceptor added	NO_3^-+NO_2^-	NO_3^-+N_2O	NO_2^-+N_2O	NO_3^-+NO_2^-+N_2O
Added concentration	30+30	30+30	30+30	30+30+30
Total NOx concentration	60	60	60	90
Data set 3	**H**	**I**	**J**	**K**
Electron acceptor added	NO_3^-+NO_2^-	NO_3^-+N_2O	NO_2^-+N_2O	NO_3^-+NO_2^-+N_2O
Added concentration	15+15	15+15	15+15	10+10+10
Total NOx concentration	30	30	30	30

Concentration unit: mg-N/L.

denitrifying bacteria and key genes involved in the electron transfer system, which could be related to significant variations in extracellular polymeric substance composition.

From Fig. 5, NO_3^-, NO_2^- and N_2O exhibited a distinct reduction sequence, i.e., electrons were first utilized by NO_3^- for its reduction and then NO_2^- levels showed a decreasing trend as NO_3^- was nearly depleted, followed by N_2O. On top of this phenomenon, NO_2^- represented an apparent accumulation during the degradation of NO_3^-, as was the relationship between NO_2^- and N_2O. Especially, the presence of NO_2^- caused N_2O to initially accumulate at the start of the test (i.e., 0–1 h and 0–3 h in Fig. 5**C** and 5**D**, respectively), followed by its subsequent consumption (i.e., 1–3 h and 3–4 h in Fig. 5**C** and 5**D**, respectively). This was inconsistent with the results observed in previous co-diffusion biofilm systems (Pan et al., 2019), which may be attributed to the counter--diffusion structure of the PCL-driven SPD system. In counter-diffusion biofilms (Chen et al., 2019), the flow directions of NO_x and carbon sources were opposite, causing a delay in the flow of electrons from the upstream electron pool to the downstream electron pools, further hindering the flow of electrons toward *Nir* and *Nos*, subsequently slowing down the NO_2^- and N_2O reduction rate. It is worth noting that the addition of NO_2^- and/or N_2O at the same concentration accelerated the NO_3^- reduction rate, which indicated that the addition of various NO_x promoted the utilization of PCL by microorganisms (Zhang et al., 2022a), thus releasing more electrons and increasing the NO_3^- reduction rate (Liu et al., 2019). Similarly, the presence of NO_2^- with N_2O also increased the NO_2^- reduction rate. However, the NO_2^- reduction rate was reduced when NO_3^- was present simultaneously.

Compared to Fig. 5 (i.e., schemes d-F), in Fig. 6 (i.e., schemes H-K), the reaction time was reduced to within 1.5–2 h after the concentration of each NO_x profiles in each scheme decreased by half. Similarly, no significant change of NO_x reduction sequence was observed (Fig. 6), indicating that the decreasing N_2O reduction rate was mainly attributed to the electron competition between the upstream and downstream electron pools within the counter-diffusion biofilm, rather than the diffusion rate of NO_x from outer to inner layer in the aqueous phase. In addition, under the condition of the same concentration of total NO_x-N, the total nitrogen removal duration of single NO_x schemes was 1.5–2 times as long as that of multiple NO_x schemes. This may be because even if the total NO_x demonstrated the same level (30 mg-N/L), multiple NO_x types can still stimulate the PCL to release more electrons, thereby simultaneously performing the reduction reaction. This result was different from that of biofilm systems that initially feed sufficient carbon sources, because PCL-driven SPD systems can continuously supply sufficient carbon sources from the inner layer of the biofilm (Zhang et al., 2022a). Therefore, PCL-driven SPD system can better solve the dilemma

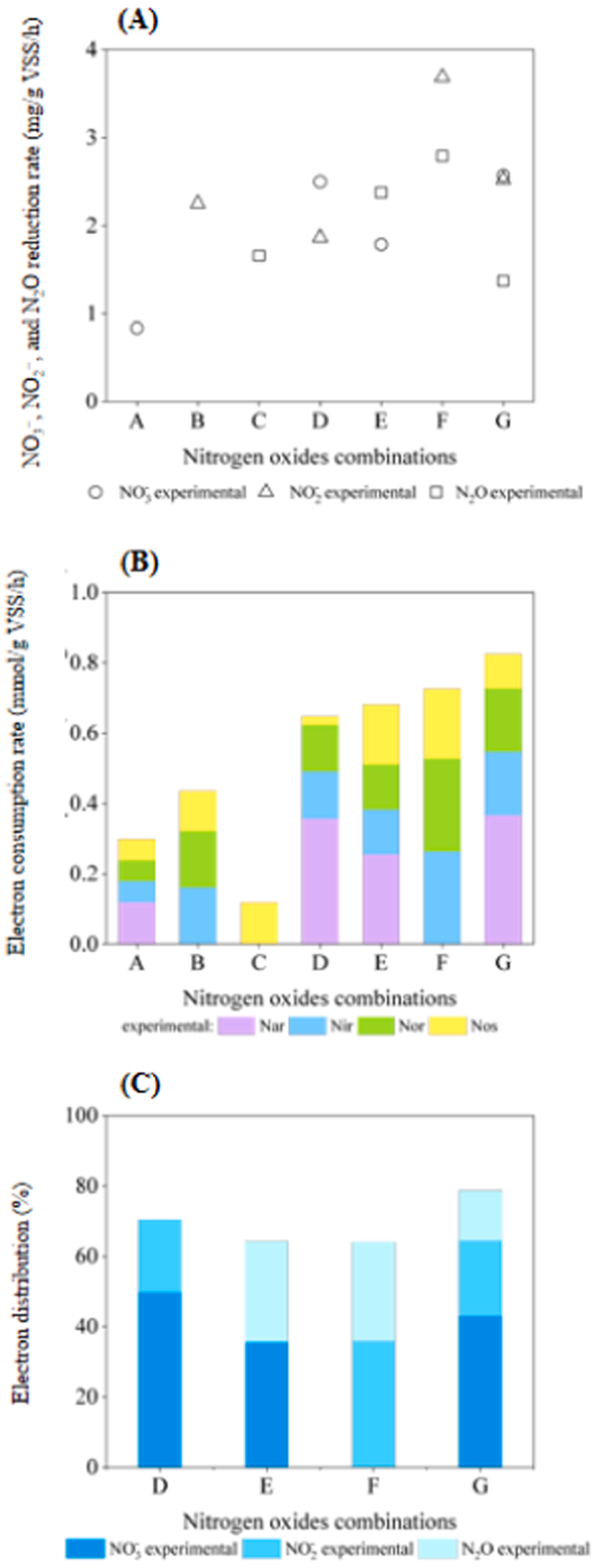

Fig. 3. NO_3^-, NO_2^- and N_2O net reduction rates (A), electron consumption rates by *Nar, Nir, Nor*, and *Nos* (B), percentages of electrons distributed to the added electron acceptors under addition schemes D, E, F, G (C).

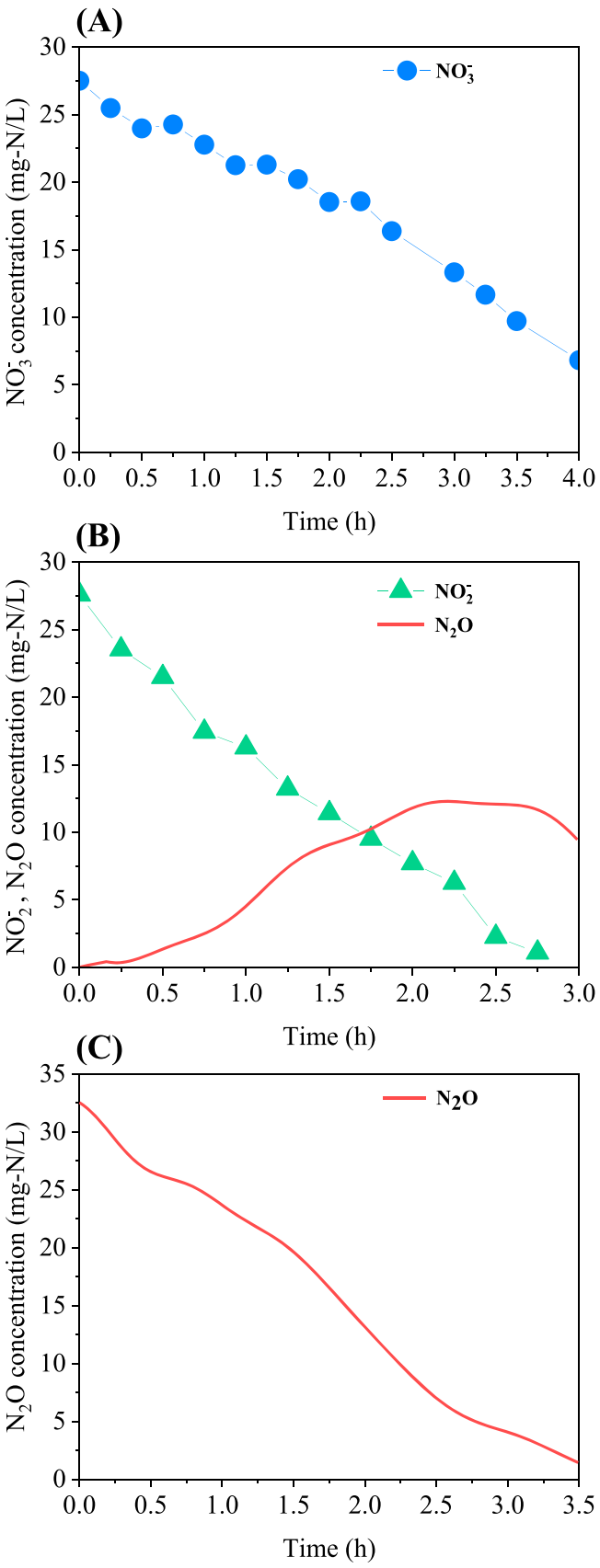

Fig. 4. The variations of NO_3^-, NO_2^- and N_2O concentrations in schemes A (A), B (B) and C (C).

of decreasing NO_x reduction rate caused by electron competition and insufficient carbon source in multiple NO_x schemes. However, the N_2O accumulation cannot be avoided simultaneously. For instance, under the condition of the total NO_x level at 30 mg-N/L, the maximum N_2O accumulation in schemes H and K reached 12.3 and 14.2 mg-N/L, respectively, primarily due to the inevitable NO_2^- accumulation. Fortunately, at the 2 h, the N_2O concentrations in both schemes H and K decreased to below 2.5 mg-N/L, whereas in scheme C (i.e., sole N_2O addition), the N_2O concentration remained at 12.8 mg-N/L. These results clearly demonstrated that the PCL-driven SPD system was effective in alleviating N_2O emissions for treating wastewater containing multiple NO_x. At WWTPs, the actual municipal wastewater was often discharged in the form of multiple NO_x simultaneously (van Dijk et al., 2021). Therefore, PCL-driven SPD systems were advantageous in reducing total nitrogen removal.

2.4. Microbial analysis

The surface sludge of PCL-driven biofilm on day 85 (R1) and day 180 (R2) were obtained and the microbial communities were analyzed. The relative abundance of bacterial populations at the phylum level was characterized in **Fig. S1**, the main microbial group with N_2O emission potential was *Proteobacteria* with 58.39 % and 40.86 % in R1 and R2, respectively, followed by *Bacteroidota* with 22.46 % and 33.31 % in R1 and R2, respectively. 33.31 % in R1 and R2, respectively. *Proteobacteria* was dominant in the whole community and its important role in organic matter and denitrification (Shen et al., 2013). *Bacteroidota* can play a role in the decomposition of macromolecules in wastewater treatment (Shen et al., 2020), and their coexistence in the system contributes to the hydrolysis of PCL. According to the release mechanism of solid carbon sources, hydrolytic enzymes were required to first break down macromolecules into small molecules that can be utilized by microorganisms, and the hydrolysis process was also considered as an important rate-limiting step. At the genus level, the dominant taxon was *unclassified_f_Comamonadaceae* with 46.39 % and 31.41 % in R1 and R2, respectively (**Fig. S2**). *Comamonadaceae* were commonly detected in solid phase denitrification systems responsible for polymer degradation, and were the main PCL degrading denitrifying bacteria with the ability to reduce NO_3^- to NO_2^-(Wu et al., 2013). These results indicated that the carbon-nitrogen counter-diffusion biofilm system maintained stable carbon source release and nitrogen conversion states, providing a stable microbial environment that ensured the reliability of biochemical tests results.

3. Conclusion

In the carbon and nitrogen counter-diffusion biofilm system, the NO_3^- reduction rate was the fastest in the multiple NO_x schemes, where the total electron consumption rate was significantly higher than in the sole NO_x addition schemes. The fiercer electron competition was obtained between the upstream and downstream electron pool, resulting in inevitable N_2O accumulations. The NO_x sequential reduction (NO_3^-→NO_2^-→N_2O) was clearly observed under different nitrogen loading conditions, which further indicated that carbon release from solid carbon sources was a non-limiting factor. The *Comamonadaceae* was the dominant species at the genus level for denitrification.

4. Materials and methods

4.1. Reactor startup and continuous operation

PCL stands out as a promising biodegradable polymer due to its considerable carbon source release rate and denitrification efficiency as well as high bioavailability (Zhang et al., 2022a). Therefore, PCL was selected as biofilm carriers and external electron donors in this study. PCL exhibited a spherical pellets shape with a diameter of ca. 3 mm, a

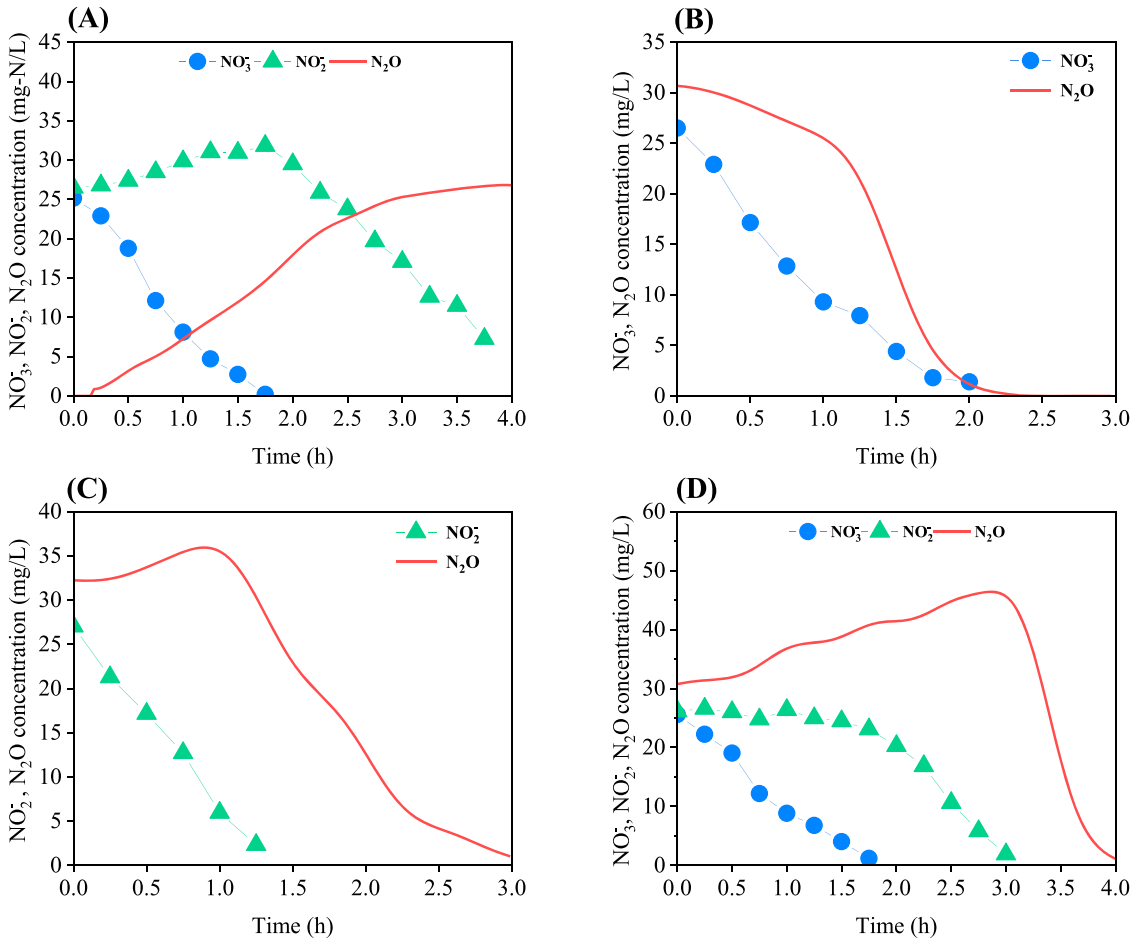

Fig. 5. The variations of NO_3^-, NO_2^- and N_2O concentrations in schemes D (A), E (B), F (C) and G (D).

bulk density of 0.78 g/mL, a real density of 1.15 g/mL, and an average molecular weight of 50,000 Da A laboratory-scale up-flow SPD cylindrical reactor was operated at 23–25 °C room temperature. The reactor was made of polyvinyl chloride, 36 cm in height, 6 cm in inner diameter, and 1.0 L in effective volume.

The reactor was packed to a filling ratio of 75 % with PCL pellets and inoculated with activated sludge from a secondary sedimentation tank. The reactor was wrapped in sunshade cloth to eliminate the possible proliferation of algae (Chu and Wang, 2013). The HRT of reactor was 3 h, and the influent pH was approximately controlled at 7.5–8. The reactor was continuously loaded with synthetic wastewater containing 50 mg-N/L NO_3^-. The composition and proportion of synthetic wastewater and trace elements were consistent with previous studies and presented in **Table S1** (Zhang et al., 2022b). The reactor was operated for more than six months.

4.2. Batch tests

4.2.1. Batch reactor setup

After over six months of operation, stable NO_3^- removal efficiency and microbial biomass were obtained in the reactor, and a dense biofilm was formed on the surface of PCL pellets. Before batch tests, to eliminate the effects of NO_x compounds and organic carbon that may remain in the reactor, it is necessary to stop the continuous feed and drain the liquid from the reactor in advance as well as wash the biofilm and PCL pellets 2–3 times. Subsequently, the reactor was modified to an internal circulation mode. To be specific, a peristaltic pump was used to connect the reactor outlet to the inlet during a batch test, with the nitrogen-containing wastewater in the reactor internally circulated from bottom to top. Finally, the synthesis wastewater was injected into the reactor until no headspace was left. The entire batch tests lasted for approximately 3–4 h

4.2.2. Batch test operation

In order to provide the reactor with anoxic conditions in all batch tests, the mixed liquor was sprayed with N_2 beforehand up to 20 min. The reactor was sealed to ensure that N_2O remained in the liquid phase. According to the addition scheme of nitrogen compounds in **Table S2**, NO_3^- and NO_2^- stock solutions were added to obtain various target NO_x concentrations of the mixture. The N_2O stock solution (i.e., 300 mg N/L) was freshly prepared through sparging Milli-Q water with 45 % N_2O gas for 10 min. Mixed liquor samples were collected from approximately the middle part of the reactor every 15 min by a syringe, and instantly filtered through a 0.22 μm filter and stored at 4 °C for NO_3^- and NO_2^- analysis (Yang et al., 2022). An online N_2O microsensor (N_2O-R, Unisense A/S. Aarhus, Denmark) was used to monitor liquid-phase N_2O constantly. The microsensor was calibrated before each test. The pH of each batch was controlled within the optimal range for NO_x reduction (i.e., 8.0 ± 0.1) and regulated with 1 M HCL or 1 M NaOH solution (Pan et al., 2012). According to standard methods, NO_3^- and NO_2^- concentrations were examined at the end of experiments (APHA, 1998).

4.2.3. Batch test design

11 combinations of electron compounds addition schemes (i.e., schemes A-K) were carried out in **Table S2**. To better understand the impact of the electron competition on N_2O reduction and the electron preference for different nitrogen oxide reductases in the PCL-driven SPD system, each NO_x concentration was set to 30 mg-N/L in the sole or

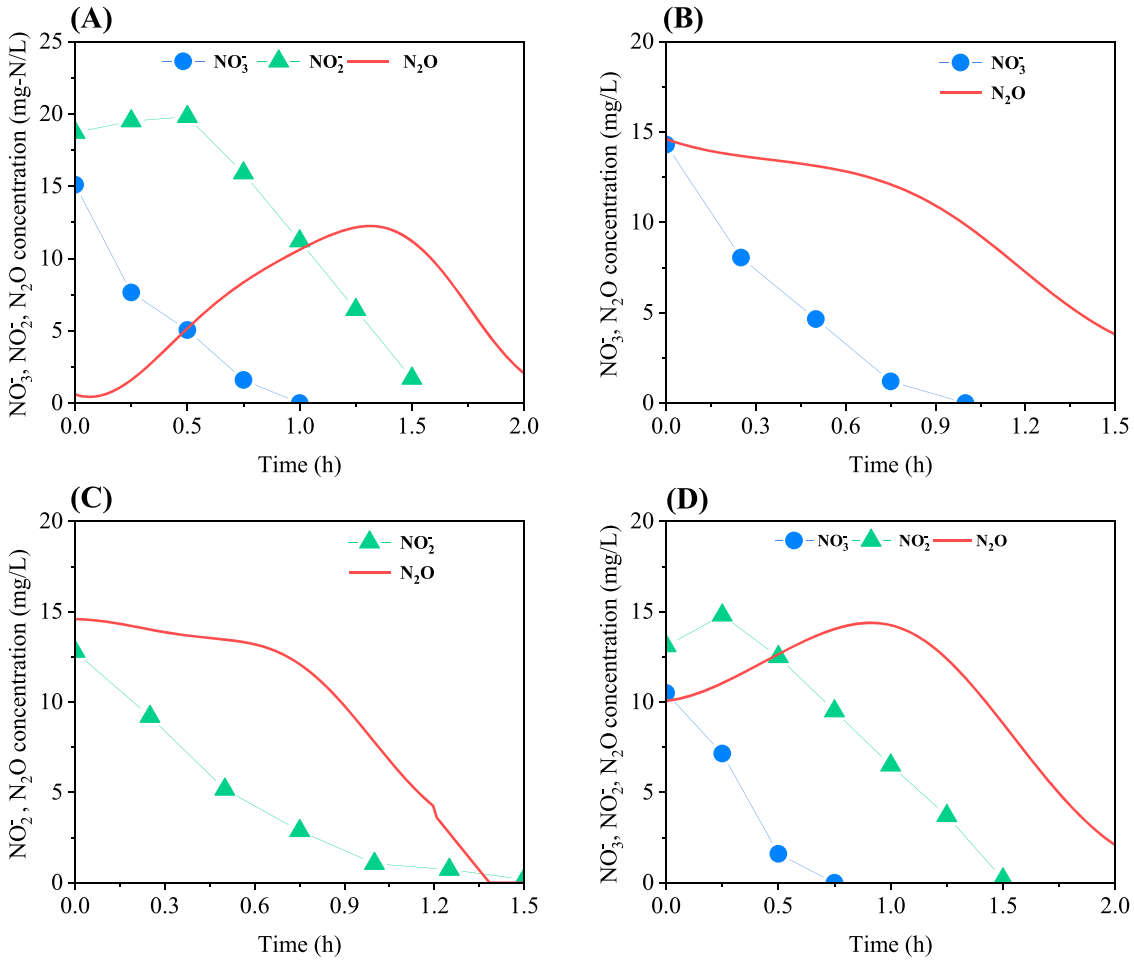

Fig. 6. The variations of NO_3^-, NO_2^- and N_2O concentrations in schemes H (A), I (B), J (C) and K (D).

multiple NO_x schemes (i.e., A-G). The variation of NO_x concentration based on electron competition was obtained from the initial 1 h of batch tests in schemes A-G (Pan et al., 2013). In addition, to further investigated the NO_x reduction and N_2O accumulation in the PCL-driven SPD system, the total NO_x concentration in the multiple nitrogen combination schemes (i.e., H-K) was adjusted to 30 mg-N/L, which was similar with the NO_x concentration of schemes A-C. The variation of NO_x concentration was obtained from the 3–4 h batch tests.

4.3. Microbial community analysis

After the biofilm on the surface of PCL particles was stabilized, a certain amount of film hanging particles was taken, and the biofilm was shed through ultrasonic treatment. The shed biofilm was collected in a centrifuge tube, concentrated and frozen for storage at -20 °C, and the microbial diversity operation and analysis were performed by 16S rRNA sequencing (Wang et al., 2024b; Wang et al., 2024c; Wang et al., 2022a). The main steps are as follows: firstly, DNA sequence extracted by Qubit ssDNA Assay using agarose gel (1 %) electrophoresis; secondly, ABI GeneAmp® 9700 PCR was used to perform PCR amplification of the V4 region of 16S rRNA gene, and the amplification primers were 515F (5 '-GTGCCAGCMGCCGCGG-3′) and 806R (5 '-GGACTACHVGG GTWTCTAAT-3′); then TruSeqTM DNA Sample Prep toolbox was used to construct Miseq library for the sequences that met the requirements (Dai et al., 2024; Guo et al., 2023); finally, paired end sequencing analysis was performed on Illumina Miseq platform according to different sample sequencing requirements.

CRediT authorship contribution statement

Yingrui Liu: Writing – original draft, Resources, Methodology, Investigation, Formal analysis, Data curation, Conceptualization. **Feng Chen:** Conceptualization. **Yanying He:** Data curation. **Yufen Wang:** Formal analysis. **Tingting Zhu:** Funding acquisition. **Yindong Tong:** Investigation. **Yingxin Zhao:** Methodology. **Bing-Jie Ni:** Software. **Yiwen Liu:** Writing – review & editing, Funding acquisition.

Declaration of competing interest

The authors declare that they have no known competing financial interests or personal relationships that could have appeared to influence the work reported in this paper.

Acknowledgements

This study was funded by National Natural Science Foundation of China through projects (No. 52470108). The authors are grateful to the research collaboration.

Supplementary materials

Supplementary material associated with this article can be found, in the online version, at doi:10.1016/j.wroa.2025.100306.

Data availability

Data will be made available on request

References

APHA (1998) Standard methods for the examination of water and wastewater. Washington DC, USA.

Chen, X., Ni, B.J., Sin, G., 2019. Nitrous oxide production in autotrophic nitrogen removal granular sludge: a modeling study. Biotechnol. Bioeng. 116 (6), 1280–1291.

Chu, L., Wang, J., 2013. Denitrification performance and biofilm characteristics using biodegradable polymers PCL as carriers and carbon source. Chemosphere 91 (9), 1310–1316.

Dai, H., Han, T., Sun, T., Zhu, H., Wang, X., Lu, X., 2021. Nitrous oxide emission during denitrifying phosphorus removal process: a review on the mechanisms and influencing factors. J. Environ. Manage. 278, 111561.

Dai, S., Guo, H., Li, Y., Hou, J., Wang, Y., Zhu, T., Ni, B.-J., Liu, Y., 2024. Application of organic silicon quaternary ammonium salt (QSA) to reduce carbon footprint of sewers: long-term inhibition on sulfidogenesis and methanogenesis. Water. Res. X. 25, 100275.

Duan, H., Zhao, Y., Koch, K., Wells, G.F., Zheng, M., Yuan, Z., Ye, L., 2021. Insights into nitrous oxide mitigation strategies in wastewater treatment and challenges for wider implementation. Environ. Sci. Technol. 55 (11), 7208–7224.

Fang, D., Wu, A., Huang, L., Shen, Q., Zhang, Q., Jiang, L., Ji, F., 2020. Polymer substrate reshapes the microbial assemblage and metabolic patterns within a biofilm denitrification system. Chem. Eng. J. 387, 124128.

Fu, X., Hou, R., Yang, P., Qian, S., Feng, Z., Chen, Z., Wang, F., Yuan, R., Chen, H., Zhou, B., 2022. Application of external carbon source in heterotrophic denitrification of domestic sewage: a review. Sci. Total Environ. 817, 153061.

Guo, H., Tian, L., Liu, S., Wang, Y., Hou, J., Zhu, T., Liu, Y., 2023. The potent effects of polyoxometalates (POMs) on controlling sulfide and methane production from sewers. Chem. Eng. J. 453, 139955.

Hatzikioseyian, A., Mendrinou, P., Kousi, P., Remoundaki, E., 2023. Modeling biological denitrification in the presence of metal ions and elevated chloride content: insights into abiotic and biotic mechanisms regulating metal bioprecipitation. J. Environ. Manage. 342, 118285.

He, X., Li, Z., Xing, C., Li, Y., Liu, M., Gao, X., Ding, Y., Lu, L., Liu, C., Li, C., Wang, D., 2023a. Carbon footprint of a conventional wastewater treatment plant: an analysis of water-energy nexus from life cycle perspective for emission reduction. J. Clean. Prod. 429, 139562.

He, Y., Li, X., Liu, Y., Guo, H., Wang, Y., Zhu, T., Tong, Y., Zhao, Y., Ni, B.-J., Liu, Y., 2024a. Biodegradable microplastics increase N2O emission from denitrifying sludge more than conventional microplastics. Environ. Sci. Technol. Lett. 11 (7), 701–708.

He, Y., Li, Y., Li, X., Liu, Y., Wang, Y., Guo, H., Hou, J., Zhu, T., Liu, Y., 2023b. Net-zero greenhouse gas emission from wastewater treatment: mechanisms, opportunities and perspectives. Renew. Sustain. Ener. Rev. 184, 113547.

He, Y., Liu, Y., Li, X., Guo, H., Zhu, T., Liu, Y., 2024b. Polyvinyl chloride microplastics facilitate nitrous oxide production in partial nitritation systems. Environ. Sci. Technol. 58 (4), 1954–1965.

Hu, Z., Liu, T., Wang, Z., Meng, J., Zheng, M., 2023. Toward energy neutrality: novel wastewater treatment incorporating acidophilic ammonia oxidation. Environ. Sci. Technol. 57 (11), 4522–4532.

Huang, M., Zhang, Y., Wu, J., Wang, Y., Xie, Y., Geng, Y., Zhang, N., Michelsen, A., Li, S., Zhang, R., Shen, Q., Zou, J., 2023. Bacillus velezensis SQR9 inhibition to fungal denitrification responsible for decreased N2O emissions from acidic soils. Sci. Total Environ 885, 163789.

Liu, Y., He, Y., Lu, Q., Zhu, T., Wang, Y., Tong, Y., Zhao, Y., Ni, B.-J., Liu, Y., 2025. Smaller sizes of polyethylene terephthalate microplastics mainly stimulate heterotrophic N2O production in aerobic granular sludge systems. Water. Res. X. 27, 100299.

Liu, Y., He, Y., Ren, S., Zhu, T., Liu, Y., 2022. Selective organic carbon enrichment influences nitrous oxide reduction by denitrifiers: electron competition insights. ACS. ES. T. Water. 2 (7), 1265–1275.

Liu, Y., Wei, D., Xu, W., Feng, R., Du, B., Wei, Q., 2019. Nitrogen removal in a combined aerobic granular sludge and solid-phase biological denitrification system: system evaluation and community structure. Bioresour. Technol. 288, 121504.

Pan, Y., Liu, Y., Peng, L., Ngo, H.H., Guo, W., Wei, W., Wang, D., Ni, B.-J., 2019. Substrate diffusion within biofilms significantly influencing the electron competition during denitrification. Environ. Sci. Technol. 53 (1), 261–269.

Pan, Y., Ni, B.-J., Bond, P.L., Ye, L., Yuan, Z., 2013. Electron competition among nitrogen oxides reduction during methanol-utilizing denitrification in wastewater treatment. Water Res. 47 (10), 3273–3281.

Pan, Y., Ye, L., Ni, B.-J., Yuan, Z., 2012. Effect of pH on N2O reduction and accumulation during denitrification by methanol utilizing denitrifiers. Water Res. 46 (15), 4832–4840.

Roy, S., Nirakar, P., Yong, N.G.H., Stefan, W., 2021. Denitrification kinetics indicates nitrous oxide uptake is unaffected by electron competition in Accumulibacter. Water Res. 189, 116557.

Shen, Q., Ji, F., Wei, J., Fang, D., Zhang, Q., Jiang, L., Cai, A., Kuang, L., 2020. The influence mechanism of temperature on solid phase denitrification based on denitrification performance, carbon balance, and microbial analysis. Sci. Total Environ. 732, 139333.

Shen, Z., Zhou, Y., Hu, J., Wang, J., 2013. Denitrification performance and microbial diversity in a packed-bed bioreactor using biodegradable polymer as carbon source and biofilm support. J. Hazard. Mater. 250-251, 431–438.

Tong, Y., Liao, X., He, Y., Cui, X., Wishart, M., Zhao, F., Liao, Y., Zhao, Y., Lv, X., Xie, J., Liu, Y., Chen, G., Hou, L.a., 2024. Mitigating greenhouse gas emissions from municipal wastewater treatment in China. Environ. Sci. Ecotechnol. 20, 100341.

van Dijk, E.J.H., van Loosdrecht, M.C.M., Pronk, M., 2021. Nitrous oxide emission from full-scale municipal aerobic granular sludge. Water Res. 198, 117159.

Wang, X., Zhang, Z., Yang, X., Wang, Y., Li, Y., Zhu, T., Zhao, Y., Ni, B.-J., Liu, Y., 2024a. Interaction of poly dimethyl diallyl ammonium chloride with sludge components: anaerobic digestion performance and adaptive changes of anaerobic microbes. Water Res. 266, 122368.

Wang, Y., Chen, F., Guo, H., Sun, P., Zhu, T., Horn, H., Liu, Y., 2024b. Permanganate (PM) pretreatment improves medium-chain fatty acids production from sewage sludge: the role of PM oxidation and in-situ formed manganese dioxide. Water Res. 249, 120869.

Wang, Y., Guo, H., Li, X., Chen, X., Peng, L., Zhu, T., Sun, P., Liu, Y., 2024c. Peracetic acid (PAA)-based pretreatment effectively improves medium-chain fatty acids (MCFAs) production from sewage sludge. Environ. Sci. Ecotechnol. 20, 100355.

Wang, Y., Sun, P., Guo, H., Zheng, K., Zhu, T., Liu, Y., 2022a. Performance and mechanism of sodium percarbonate (SPC) enhancing short-chain fatty acids production from anaerobic waste activated sludge fermentation. J. Environ. Manage. 313, 115025.

Wang, Y., Zheng, K., Guo, H., Tong, Y., Zhu, T., Liu, Y., 2022b. Unveiling the mechanisms of how vivianite affects anaerobic digestion of waste activated sludge. Bioresour. Technol. 343, 126045.

Wu, W., Yang, L., Wang, J., 2013. Denitrification using PBS as carbon source and biofilm support in a packed-bed bioreactor. Environ. Sci. Pollut Res 20 (1), 333–339.

Yang, Y., Perez Calleja, P., Liu, Y., Nerenberg, R., Chai, H., 2022. Assessing intermediate formation and electron competition during thiosulfate-driven denitrification: an experimental and modeling study. Environ. Sci. Technol. 56 (16), 11760–11770.

Zhang, S., Tang, Z., Xia, S., Jiang, Y., Li, M., Wang, B., 2022a. The intrinsic relevance of nitrogen removal pathway to varying nitrate loading rate in a polycaprolactone-supported denitrification system. Biodegradation 33 (4), 317–331.

Zhang, Z., Wang, X., Yang, X., Wang, Y., Li, X., Ding, J., Zhu, T., Sun, P., Ni, B.J., Liu, Y., 2025. Unveiling the synergistic potential of ferrate and pyrophosphate co-pretreatment enhancing anaerobic sludge fermentation: performance and mechanistic insights. Chem. Eng. J. 505, 159612.

Zhang, S., Xiao, L., Tang, Z., Zhang, X., Wang, Z., 2022b. Microbial explanation to performance stratification along up-flow solid-phase denitrification column packed with polycaprolactone. Bioresour. Technol. 343, 126066.

Zheng, M., Hu, Z., Liu, T., Sperandio, M., Volcke, E.I.P., Wang, Z., Hao, X., Duan, H., Vlaeminck, S.E., Xu, K., Zuo, Z., Guo, J., Huang, X., Daigger, G.T., Verstraete, W., van Loosdrecht, M.C.M., Yuan, Z., 2024. Pathways to advanced resource recovery from sewage. Nat. Sustain. 7 (11), 1395–1404.